Hydrometeorological application of a microwave link: 2. Precipitation

H. Leijnse,[1] R. Uijlenhoet,[1] and J. N. M. Stricker[1]

Received 21 February 2006; revised 31 May 2006; accepted 23 August 2006; published 12 April 2007.

[1] The suitability of a 27-GHz microwave link for measuring path-averaged precipitation is investigated. Theoretical analyses show that the specific attenuation of an electromagnetic signal at this frequency varies nearly linearly with the rainfall intensity, which is ideal for line-integrating instruments. The dependence of this relation on the drop size distribution and on the temperature is small, so that uncertainties in these variables do not play large roles in the estimation of rainfall intensity. Data from an experiment with a 4.89-km microwave link and a line configuration of seven tipping bucket rain gauges are used to test whether this instrument is indeed suitable for the estimation of path-averaged rainfall. Results from this experiment show that the attenuation due to wet antennas can have a significant effect on the retrieved rainfall intensity. However, when a two-parameter wet antenna correction function is applied to the link data, comparisons with the rain gauge data show that the instrument is indeed well suited for the measurement of path-averaged rainfall.

Citation: Leijnse, H., R. Uijlenhoet, and J. N. M. Stricker (2007), Hydrometeorological application of a microwave link: 2. Precipitation, *Water Resour. Res.*, *43*, W04417, doi:10.1029/2006WR004989.

1. Introduction

[2] The potential of microwave links to estimate path-averaged evaporation has been discussed by *Leijnse et al.* [2007]. The present paper deals with the estimation of path-averaged precipitation using the same instrument. This combination makes this type of instrument potentially highly suitable for both hydrological and meteorological applications.

[3] Measurement of rainfall on several spatial and temporal scales is extremely important in hydrology, especially in urban settings [e.g., *Smith et al.*, 2002; *Leijnse et al.*, 2002; *Berne et al.*, 2004] where processes on the scale of neighborhoods can be very important. *Upton et al.* [2005] propose that microwave links are ideal for measurement of rainfall for hydrological applications in urban settings [see also *Grum et al.*, 2005]. In addition to this, rainfall estimated from microwave links could be used for calibration and verification of ground-based or spaceborne radar measurements [*Rahimi et al.*, 2004; *Krämer et al.*, 2005] and for hydrologic or climate models. As such, microwave links may serve to bridge the scale gap between the traditional instruments used to measure rainfall (i.e., weather radar and rain gauges). Because of their integrating character, microwave links will suffer less from sampling errors and can measure at higher temporal resolution than rain gauges, especially at low rainfall intensities. Much can be gained from line measurements of the rainfall intensity in addition to point (rain gauges) and areal (radar) measurements.

[4] Most recent studies on rainfall estimation using microwave links focus on either dual-polarization [*Ruf et al.*, 1996] or dual-frequency [*Rincon and Lang*, 2002; *Rahimi et al.*, 2003] techniques, both yielding very promising results. In a comparison between single-frequency and dual-frequency microwave links, *Holt et al.* [2003] conclude that the suitability of single-frequency links for measuring path-averaged rainfall approaches that of dual-frequency links only at frequencies around 24 GHz owing to the fact that the relation between signal attenuation and rainfall intensity is nearly linear and relatively insensitive to variability in drop size distribution climatology and rain temperature at this frequency. The 27-GHz microwave link used in this study operates relatively close to this frequency and is therefore expected to perform reasonably well. Use of this frequency was also suggested by *Atlas and Ulbrich* [1977]. In a recent study, *Minda and Nakamura* [2005] have shown that with a 50-GHz microwave link, operating far outside the suitability range proposed by *Holt et al.* [2003], path-averaged rainfall intensity can still be estimated with reasonable accuracy.

[5] A detailed description of a microwave link (or radio wave scintillometer) is given by *Leijnse et al.* [2007]. The electromagnetic waves propagating between the transmitter and receiver of the link are affected by raindrops. A portion of the energy in these waves is absorbed or scattered by the raindrops. The sum of this absorption and scattering is what causes the receiver to detect less radiative energy than would be the case if no rain were present. The relative decrease of the power (in dB) of the propagating signal per unit distance, the specific attenuation k (dB km^{-1}), can be used to estimate path-averaged rainfall.

[6] The method by which rainfall intensity is estimated from the specific attenuation measured by the microwave link is described in section 2. The method is verified

[1]Hydrology and Quantitative Water Management, Wageningen University, Wageningen, Netherlands.

0043-1397/07/2006WR004989$09.00

experimentally using data collected in an experiment described in section 3. Conclusions will be drawn in section 4.

2. Method

[7] The microwave link signal is attenuated by raindrops in its path. Each raindrop interacts with the electromagnetic signal because its dielectric properties differ from those of the surrounding air. Because both the rainfall intensity R (mm h^{-1}) and the signal attenuation k (dB km^{-1}) depend on the number concentration and sizes of the raindrops, the two quantities can be related.

2.1. Theory

[8] The relative decrease in power between the source of an electromagnetic signal (the transmitter) and a point in space (at a distance r from this source) due to attenuation by rainfall is given by [e.g., *Battan*, 1973]

$$\frac{P(r)}{P_0} = \exp\left(-\frac{\ln(10)}{10}\int_0^r k(s)\mathrm{d}s\right), \quad (1)$$

where P_0 is the signal power without attenuation by rain. Measuring the signal power using a receiver at a distance $r = L$, the path-integrated attenuation $A_m = \int_0^L k(s)\mathrm{d}s$ (in dB) can be derived. The objective is now to estimate path-averaged rainfall intensity $\overline{R}$ from the measured path-averaged specific attenuation $\overline{k}$, using a relation between k and R.

[9] The specific attenuation and the rainfall intensity can both be computed by integrating the drop size distribution (DSD) $N(D)$ (m^{-3} mm^{-1}), weighted by appropriate functions [e.g., *Atlas and Ulbrich*, 1977]

$$k = \frac{10^{-2}}{\ln(10)}\int_0^\infty Q_{ext}(D)N(D)\mathrm{d}D \quad (2)$$

$$R = 6\times10^{-4}\pi\int_0^\infty D^3 v(D)N(D)\mathrm{d}D, \quad (3)$$

where the prefactors are related to the conversion of units, $Q_{ext}(D)$ (mm^2) is the extinction cross section of a drop with volume equivalent diameter D (mm) and $v(D)$ (m s^{-1}) is its terminal fall velocity. The $v(D)$ relation used in this paper will be that of *Beard* [1976], which is considered to be the most accurate parameterization of raindrop terminal fall velocity in still air available to date. For a 27-GHz signal, the wavelength ($\lambda \approx 11$ mm) is of the same order of magnitude as the size of the scattering particles (raindrops). Therefore Mie scattering theory [e.g., *van de Hulst*, 1957] must be used to compute $Q_{ext}(D)$, which also depends on the rain temperature and the frequency of the signal. Although the T matrix method by *Mishchenko and Travis* [1994] is the most comprehensive for the calculation of electromagnetic scattering by particles of arbitrary shape, we do not use this computationally intensive technique here. Instead, for simplicity, we use the Mie series expansion for purely spherical particles. This assumption is justified because raindrop shapes deviate little from pure spheres when their volumes are small [*Pruppacher and Klett*, 1997], which is the case for drops occurring in events in moderate climatic regions. The T matrix method does become relevant when polarimetric measurements are considered, as the difference between the horizontally and vertically polarized received signals is due to the nonsphericity (oblateness) of the drops.

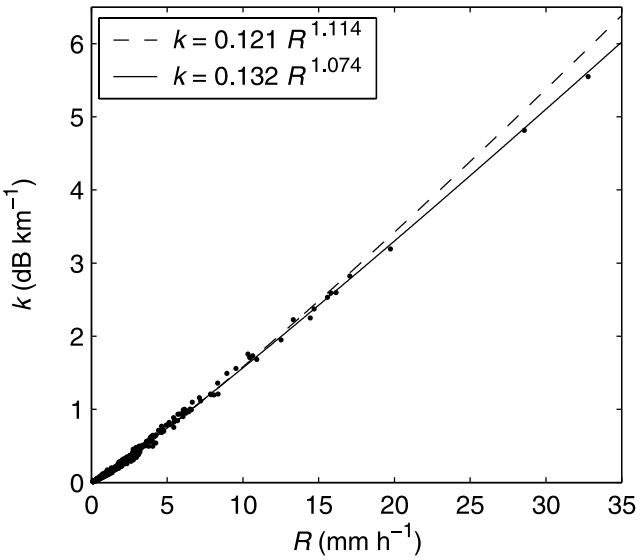

Figure 1. Specific attenuation as a function of rainfall intensity for the drop size data collected by *Wessels* [1972] for $T = 288.15$ K and a signal frequency of 27 GHz. Power law fits (dashed line, linear fit of the logarithms; solid line, nonlinear fit) to these data are also shown.

2.2. The *k*-*R* Relation

[10] As has been shown by many in the past [e.g., *Atlas and Ulbrich*, 1977; *Olsen et al.*, 1978], the k-R relation can be approximated by a power law

$$k = aR^b. \quad (4)$$

Figure 1 shows the k and R values calculated for a rain temperature of $T = 288.15$ K and at a frequency of 27 GHz using the 446 drop size distributions (where $R > 0.1$ mm h^{-1}) measured by *Wessels* [1972] in the period between 3 January 1968 and 13 March 1969 in De Bilt, Netherlands. Two power laws are also shown in Figure 1, one resulting from the linear fit of $\ln(k)$ to $\ln(R)$ and the other resulting from a nonlinear power law fit of k to R. Both regressions were based on a least squares criterion. It can be seen that the relation between k and R is nearly linear for these data, and that in any case the exponent of this power law relation is significantly closer to one than those of power law relations used for remote sensing of rainfall using weather radar [*Smith and Krajewski*, 1993]. In the remainder of this paper only nonlinear least squares fits will be used as these assign more weight to the higher rainfall intensities.

[11] *Olsen et al.* [1978] list the coefficients and exponents of power law approximations of the relations between specific attenuation and rainfall intensity for different frequencies, temperatures and classically used drop size distribution climatologies. Table 1 gives the results of linearly interpolating the listed values of the coefficients and exponents for 25 GHz and 30 GHz, at rain temperatures of 263 K, 273 K and 293 K. The exponents in Table 1 are all relatively close to 1, also indicating a nearly linear k-R relation.

Table 1. Coefficients a and Exponents b for Different Power Law Relations Between Specific Attenuation k and Rainfall Intensity R at 27 GHz for Different Rain Temperatures and for Different Drop Size Distribution Climatologies[a]

	T = 263 K		T = 273 K		T = 293 K	
	a	b	a	b	a	b
LP_L	0.132	1.078	0.128	1.081	0.135	1.063
LP_H	0.168	1.010	0.170	1.003	0.177	0.986
MP	0.153	1.054	0.147	1.062	0.153	1.051
J-T	0.215	0.863	0.213	0.860	0.218	0.847
J-D	0.116	0.994	0.103	1.037	0.094	1.117
W	0.125	1.104	0.126	1.097	0.135	1.066

[a]Values of a and b are interpolated from *Olsen et al.* [1978]. LP_L, *Laws and Parsons* [1943] distribution for low rainfall intensities (1.27–50.8 mm h^{-1}); LP_H, *Laws and Parsons* [1943] distribution for high rainfall intensities (25.4–152.4 mm h^{-1}); MP, *Marshall and Palmer* [1948] distribution; J-T, *Joss et al.* [1968] distribution for thunderstorms; J-D, *Joss et al.* [1968] distribution for drizzle. Also shown are values of a and b calculated using the drop size distributions measured in De Bilt, Netherlands, by *Wessels* [1972] (W).

[12] The near linearity of the k-R relation for different drop size distributions is the result of the fact that the integrands of equations (2) and (3) have similar shapes. This implies that the k-R relation should be nearly independent of the DSD. To demonstrate this, we have plotted $g_k(D)$ and $g_R(D)$ in Figure 2, which are normalized versions of the integrands of equations (2) and (3)

$$g_k(D) = \frac{10^{-2}}{k\ln(10)} Q_{ext}(D) \tag{5}$$

$$g_R(D) = \frac{6\times 10^{-4}\pi}{R} D^3 v(D). \tag{6}$$

Note that the shapes of these lines are independent of the DSD, as $N(D)$ is only used in the normalization.

[13] As a measure of the relative importance of the different regions of diameters, we have also plotted the exponential drop size distribution

$$N(D) = N_0 e^{-\Lambda D}, \tag{7}$$

with $N_0 = 8000\ \mathrm{m^{-3}\ mm^{-1}}$ [see *Marshall and Palmer*, 1948] and $\Lambda = 2.0\ \mathrm{mm^{-1}}$ (corresponding to a rainfall intensity of $R = 34.2\ \mathrm{mm\ h^{-1}}$). This DSD has also been used to compute k in equation (5) and R in equation (6) for Figure 2.

[14] From Figure 2, the conclusion can be drawn that the integrands are indeed similar for k and R for raindrop diameters between 0.1 and 4.0 mm, and that the region of drop sizes where they start to deviate is a region where $N(D)$ is negligible. This is the reason for the near linearity of the k-R relation. It can also be seen that the $Q_{ext}(D)$ and the $v(D)$ relations can be approximated by power laws (the graphs on log-log scales are nearly linear), and that the difference between the exponents of these power laws is approximately 3 (the slopes in the log-log graphs are nearly equal, see also equations (2) and (3)). *Atlas and Ulbrich* [1977] based their conclusion that the k-R relation is nearly linear on similar observations.

[15] Because the extinction cross section is temperature-dependent, the analysis of Figure 1 can be repeated for different rain temperatures. The coefficients and exponents of the power law fits to the data of *Wessels* [1972] are plotted as a function of the temperature T in Figure 3. It can be seen that the ranges of values of both a and b are limited in the wide range of rain temperatures (263.15 K $\leq T \leq$ 313.15 K) shown here. Comparing the range of values of a and b to those listed in Table 1 leads to the conclusion that the temperature is not a very important factor in this analysis as compared to the DSD climatology. Furthermore, the exponent b is close to 1, so that the k-R relation is nearly linear over this range of temperatures. It must be noted, however, that when the rain temperature drops below 273.15 K, the precipitation may be partly frozen, considerably changing the extinction coefficient $Q_{ext}(D)$. Frozen precipitation is outside the scope of this paper, but it is important to realize that it can occur and significantly affect the k-R relation.

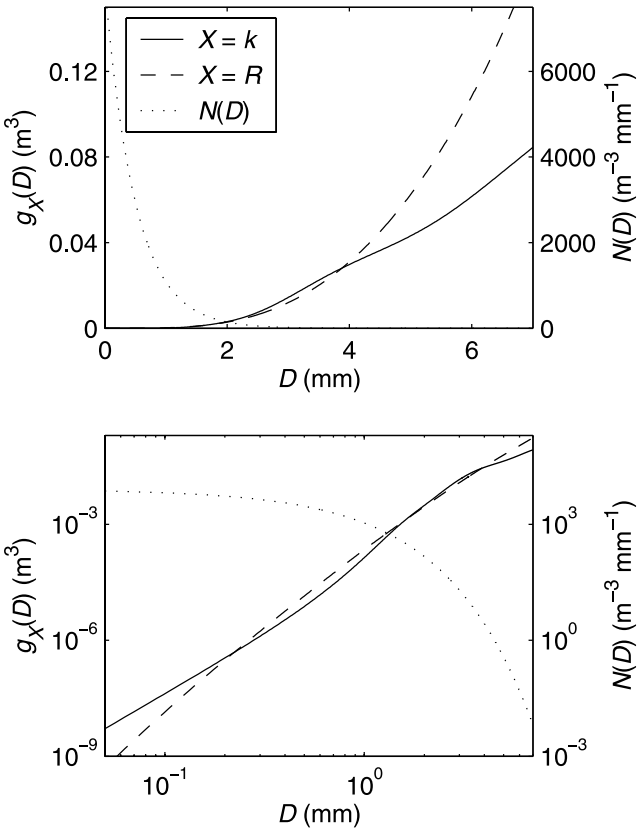

Figure 2. Normalized DSD-independent parts of the integrands of the integrals used to compute the specific attenuation and the rainfall intensity, on (top) linear and (bottom) logarithmic scales. Also shown is the exponential DSD (with N_0 = 8000 and Λ = 2.0 $\mathrm{mm^{-1}}$).

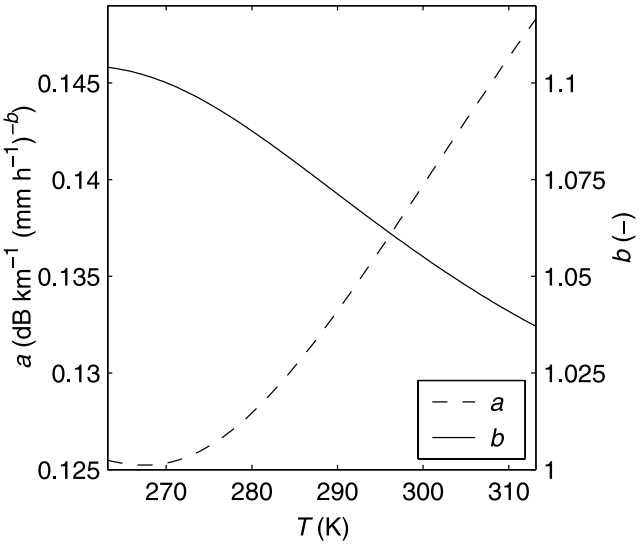

Figure 3. Temperature dependence of the coefficient a and exponent b of the power law approximation of the k-R relation for the drop size distributions measured by *Wessels* [1972].

[16] An important result of the near linearity of the k-R relation ($k \approx cR$) is that the path-integrated attenuation A_m can be directly related to the path-averaged rainfall intensity $\overline{R}$ (see equation (1))

$$A_m = \int_0^L k(s)\mathrm{d}s \approx c\int_0^L R(s)\mathrm{d}s = cL\overline{R}.$$

[17] In the remainder of this paper, the k-R relation based on the DSDs measured by *Wessels* [1972] (see Figure 1) will be used. This is done because it is assumed to be representative of the DSDs occurring in the Netherlands, where the experimental verification (see section 3) was carried out. However, because the dependence of the k-R relation at 27 GHz on the DSD is limited, this choice should not greatly influence the results.

3. Experimental Verification

[18] The same microwave instrument as the one used to verify the estimation of evaporation [*Leijnse et al.*, 2007] was used in an experiment a year later to test its potential to estimate precipitation. The results of this experiment will be presented in this section. The bars over $\overline{R}$ and $\overline{k}$ to denote path averages will be dropped in this section for simplicity of notation.

3.1. Experimental Setup

[19] An experiment with a 27-GHz microwave link was conducted between the towns of Rhenen and Wageningen (4890 m), The Netherlands (see Figure 4). In the period in which the experiment took place, from 28 May 1999 to 23 July 1999, over 120 hours of rainfall occurred in 25 separate events.

[20] The microwave link was manufactured by the Eindhoven University of Technology, and on loan from the Horticultural Research Institute of New Zealand [*Green et al.*, 2000]. The antennas of the system both have diameters of 0.6 m, and were mounted 46 m (transmitter) and 19 m (receiver) above the terrain. The received signal is fed through a logarithmic amplifier, after which it is low-pass filtered with a cutoff frequency of 10 Hz. The resulting signal is sampled at a rate of approximately 18 Hz. Hourly averages of meteorological variables like temperature and humidity were measured at the meteorological station of Wageningen University, operated by the Meteorology and Air Quality Group (see Figure 4).

[21] A line configuration of seven tipping bucket rain gauges was used to independently estimate path-averaged rainfall intensity. The manufacturer-supplied nominal tipping volume of the gauges is approximately 0.2 mm, which was verified by dynamic calibration after the experiment. Figure 4 shows the locations of these gauges relative to the microwave link signal path. The rainfall intensity measured by the gauges is averaged according to their distance to the nearest working neighbors or to the transmitter or receiver (see Table 2)

$$R = \sum_{i=1}^{N} w_i R_i, \tag{8}$$

where R_i is the rainfall intensity measured by gauge i and N is the number of operational gauges. The weights of each of the operating gauges w_i is given by

$$w_i = \frac{1}{2L}(x_{i+1} - x_{i-1}), \tag{9}$$

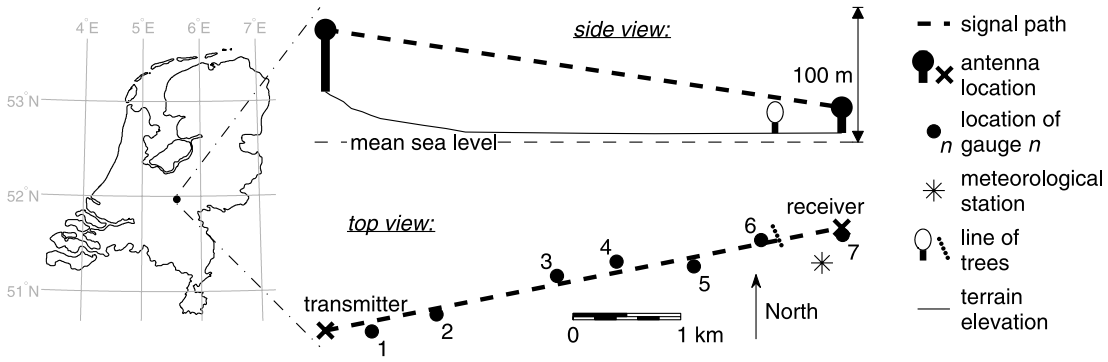

Figure 4. Location of the experimental site within the Netherlands and a top and a side view of the study area.

Table 2. Period During Which Data Are Used and Distance From the Transmitter Along the Microwave Link Signal Path x of the Seven Gauges[a]

Gauge	Operational Period	x, km
1	29 May 1999 to 24 July 1999	0.43
2	29 May 1999 to 12 June 1999	1.03
3	none (vandalism)	2.20
4	29 May 1999 to 20 June 1999	2.73
5	18 June 1999 to 24 July 1999	3.46
6	24 June 1999 to 24 July 1999	4.14
7	29 May 1999 to 24 July 1999	4.89

[a]See Figure 4.

where x_i is the position of gauge i, $x_0 = 2x_{tr} - x_1$ (x_{tr} is the location of the transmitter), $x_{N+1} = 2x_{rec} - x_N$ (x_{rec} is the location of the receiver) and L is the link length (note that $x_{tr} = 0$ m and $x_{rec} = L$). This average is assumed to be representative for the path-averaged rainfall intensity.

[22] Figure 4 shows that a line of trees is located close to the signal path. This caused the signal to fluctuate due to reflections of the signal off the leaves and branches moving in the wind, masking the signal fluctuations caused by turbulent eddies moving through the signal path. Therefore, unfortunately, the data obtained in this experiment could not be used to estimate evaporation [see *Leijnse et al.*, 2007]. Because the tops of the trees are just outside the first Fresnel zone of the link, they do not affect the mean level of the signal and the experimental data can still be used for testing the potential of a microwave link for the estimation of precipitation.

3.2. Rain Gauge Measurements

[23] The internal clocks of the different gauges were observed to be a little slow, so that precise timing of the onset of the rainfall events is not possible. However, the time signature of the events that occurred during the measurement period is not much affected by this. The gauge clocks are corrected manually by comparing the time indicated by the gauge to the actual time when the gauges were checked in the field during the experiment. It is assumed that the clock speed has not changed between these checks, so that the correction can be carried out by linear interpolation. The gauge results are then checked for each rainfall event against the other gauges and against the microwave link signal. If this timing adjustment is judged not to be accurate for a particular gauge, the data of this gauge is disregarded for the event. Table 2 shows the periods during which the data has been used for each of the gauges, along with information of their positions along the signal path of the microwave link. The uncertainty in the timing of the resulting averaged rainfall intensity is estimated to be approximately 90 s, based on the typical magnitude of the deviations between gauge clocks and the actual time at checks in the field.

[24] Because of the uncertainty in the timing of the gauges, both the rainfall intensity measured by the gauges and the signal attenuation measured by the microwave link are averaged over 180 s (3 min). Figure 5 shows the time series of the rainfall intensity of the individual gauges, the resulting weighted average and the 3-min averaged rainfall intensity for a portion of one particular event. It can be seen from this figure that the spatial and temporal variability of the rainfall can be significant. Therefore the average of the point measurements of the gauges may not always represent the true path average of the rainfall intensity.

3.3. Microwave Link Measurements

[25] The absorption by atmospheric constituents is neglected here except for that caused by water vapor. The signal is corrected for this using the relation given by *Ulaby et al.* [1981, chapter 5]. The attenuation by water vapor k_{H_2O} is calculated using hourly averaged values of atmospheric variables (linearly interpolated in time) measured at the meteorological station (see Figure 4). The voltage measured by the receiver V (V) is then corrected according to

$$V_Q = V - k_{H_2O} L \left(\frac{\partial V}{\partial A} \right), \tag{10}$$

where $\frac{\partial V}{\partial A} = -0.0573$ V dB^{-1} (A is the path-integrated attenuation) was obtained by laboratory calibration of the instrument. The subscript Q denotes that the voltage has been corrected for water vapor.

[26] Other effects due to slowly varying atmospheric variables include anomalous propagation, multipath propagation, convergence/divergence of the beam, and reflection of the signal off discontinuities in the temperature or humidity profile or the terrain below the link [*Herben*, 1984]. However, no profiles of the atmosphere were measured during the experiment, so that we cannot correct for this. *Herben* [1984] has shown that the effects of these phenomena are only important if the heights of the transmitter and receiver are nearly equal, so that this will not play a major role in this experiment. *Ruf et al.* [1996] show that the advantage of using the difference between the attenuation of signals at two different polarizations is that each signal propagates through the same atmosphere, and therefore the difference is not affected by factors other than rain itself. The same could be said for the difference between

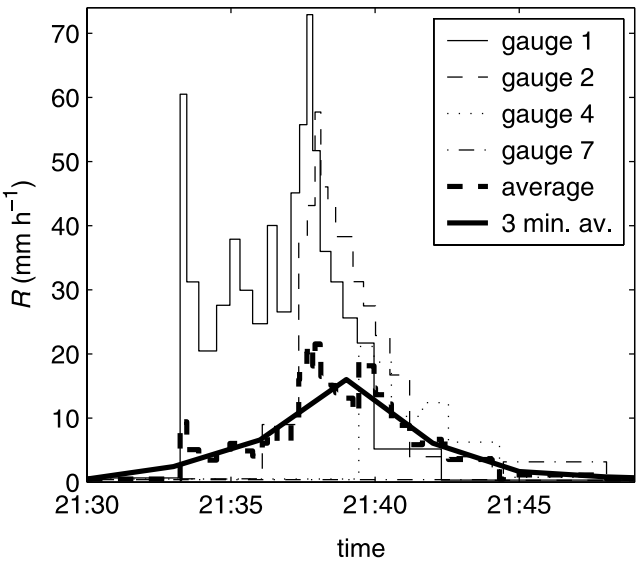

Figure 5. Time series of the rainfall intensities recorded by the gauges operating on 29 May 1999. Also shown are the resulting weighted average and 3-min averaged rainfall intensities.

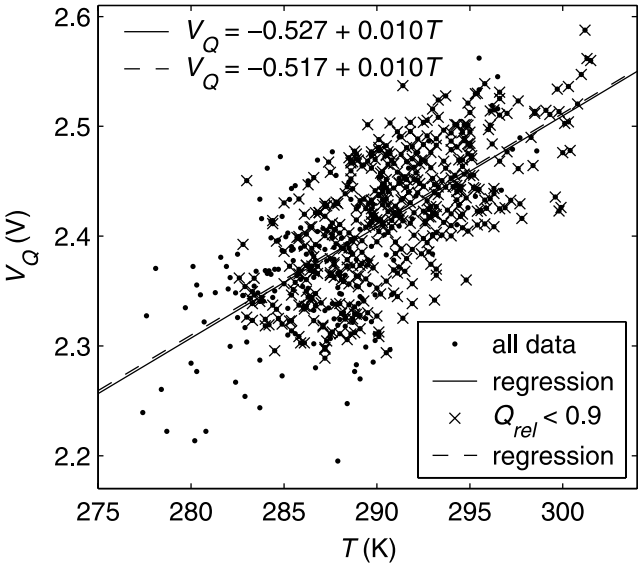

Figure 6. Hourly averaged humidity-corrected output voltage V_Q measured during dry periods plotted against the hourly averaged temperature T. Regression ($V_Q = c + dT$) analyses shown are for all data (611 points; $c = -0.527$ V, $d = 0.0101$ V K^{-1}, and $r^2 = 0.46$) and for the hours with $Q_{rel} < 0.9$ (434 points; $c = -0.517$ V, $d = 0.0101$ V K^{-1}, and $r^2 = 0.44$).

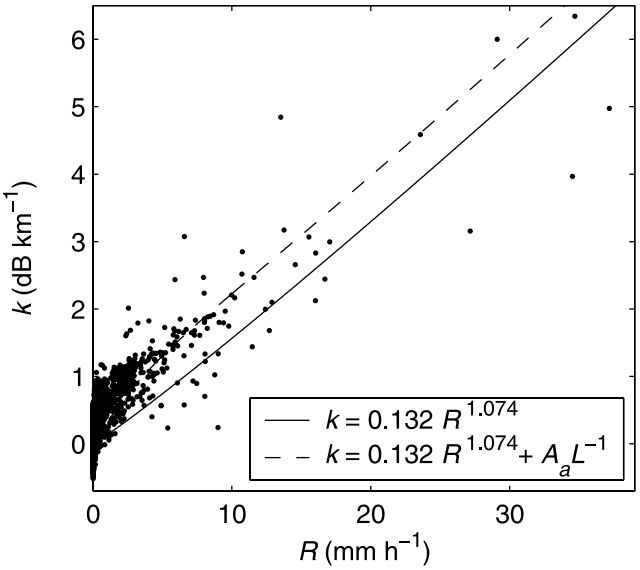

Figure 8. Comparison of the rainfall intensity measured by the gauges and the specific attenuation measured by the microwave link. Also shown are the power law obtained from Figure 1 and the result of the regression analysis of the wet antenna correction function (see equation (13)).

two signals with different frequencies [e.g., *Holt et al.*, 2003].

[27] Because the microwave instrument was manufactured as a scintillometer, no particular attention was paid to keeping the power of the signal stable over longer periods of time. This means, for example, that the gain of the amplifiers used may be temperature-dependent. *Ruf et al.* [1996] argue that using a single location for the transmitter and the receiver with a corner reflector removes this problem, as the electronics used are all exposed to the same outside conditions. However, in this case, a temperature correction to the signal (derived during dry weather) for the amplifier gain had to be applied. The magnitude of this correction is determined using a linear regression on the hourly averaged corrected output voltage V_Q (V) measured during dry periods (i.e., at least one hour removed from any rainfall measured by the gauges). Figure 6 shows the result of the linear regressions on all data and on the data for which the hourly averaged relative humidity Q_{rel} (dimensionless) was smaller than 90%. The reason for this distinction is the fact that fog and wet antennas, which only occur at high relative humidity, may cause additional attenuation. It can be seen from Figure 6 that the results of both linear regression analyses are very similar, and that the scatter is significant (coefficients of determination r^2 are relatively small). We use the regression results for $Q_{rel} < 0.9$ for the temperature correction of the signal

$$V_{QT} = V_Q - c - dT, \tag{11}$$

with $c = -0.517$ V and $d = 0.0101$ V K^{-1} (see Figure 6).

[28] The results of these corrections to the signal in dry periods can be seen in Figure 7, where the probability density functions $f_V(V)$ of $V - \overline{V}$, $V_Q - \overline{V_Q}$ and V_{QT} have been drawn ($\overline{V}$ denotes the mean of V). It can be seen that the effect of the temperature correction is much more significant than that of the water vapor attenuation correction. The specific attenuation k is estimated using this corrected voltage V_{QT} according to

$$k = \frac{V_{QT}}{L\left(\frac{\partial V}{\partial A}\right)}. \tag{12}$$

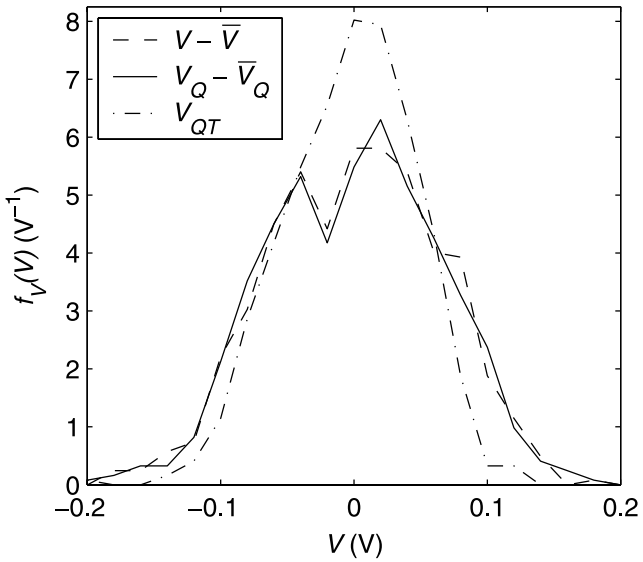

Figure 7. Probability density functions $f_V(V)$ of the raw voltage V, the water vapor attenuation-corrected voltage V_Q, and the temperature-corrected voltage V_{QT}, where the first two are shifted by their respective means.

3.4. Link-Gauge Comparison

[29] The rain gauge and microwave link data are divided into 25 separate events, starting 1 hour before and ending

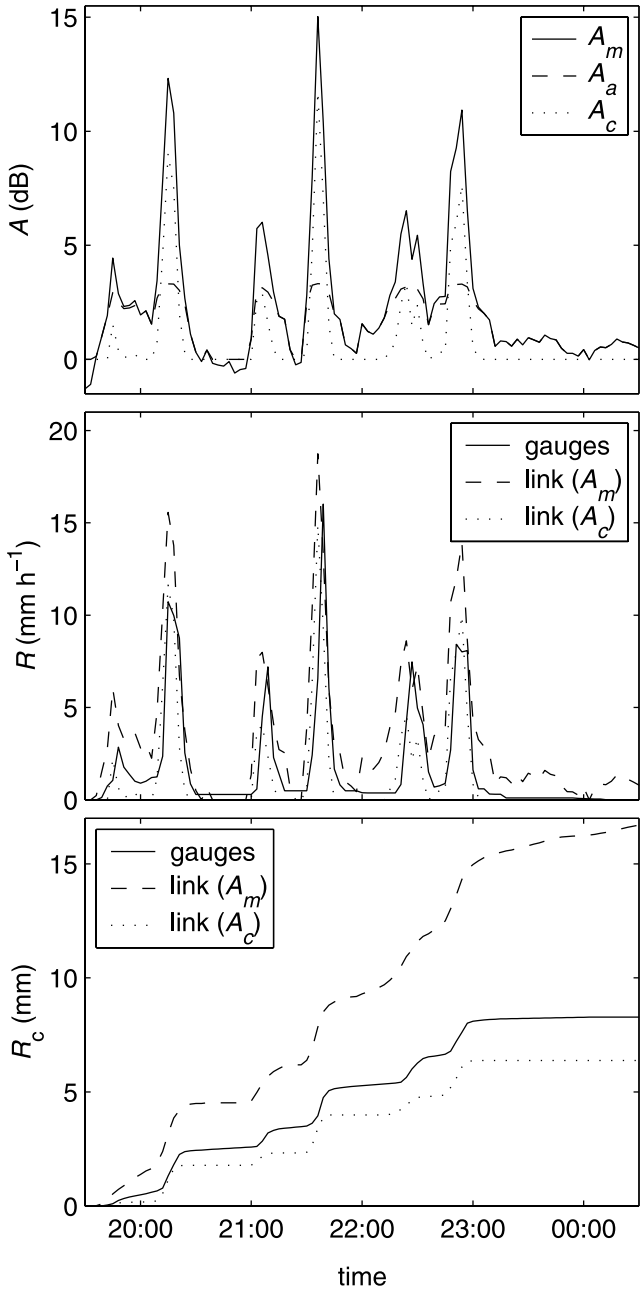

Figure 9. (top) Measured attenuation (A_m), rainfall intensity, and cumulative rainfall measured by the link, (middle and bottom) compared to the rainfall measured by the gauges. Also shown are the wet antenna attenuation (A_a) and its correction (A_c) on 29 May 1999.

1 hour after a rainfall event measured by any of the operating gauges. When 3-min averages are taken, this yields 165 hours and 30 min (3310 points) of data, of which 119 hours and 54 min (2398 points) contain rainfall. Figure 8 shows the 3-min averaged specific attenuation k as a function of the 3-min averaged rainfall intensity R, with the power law estimated from Figure 1 ($a = 0.132$ dB km^{-1} (mm h^{-1})$^{-b}$, $b = 1.074$). It can be seen that the specific attenuation is larger than expected at low rainfall intensities. This may be explained by the fact that the water films on the antennas cause additional attenuation when they become wet, which has been shown by *Kharadly and Ross* [2001] to be a significant effect.

[30] Wet antenna correction algorithms like that described by *Kharadly and Ross* [2001] and extended by *Minda and Nakamura* [2005] for slow drying of antennas can only be applied here by using the rain gauge data because the antennas were not calibrated for water film attenuation. The attenuation caused by the wet antennas A_a (dB) as a

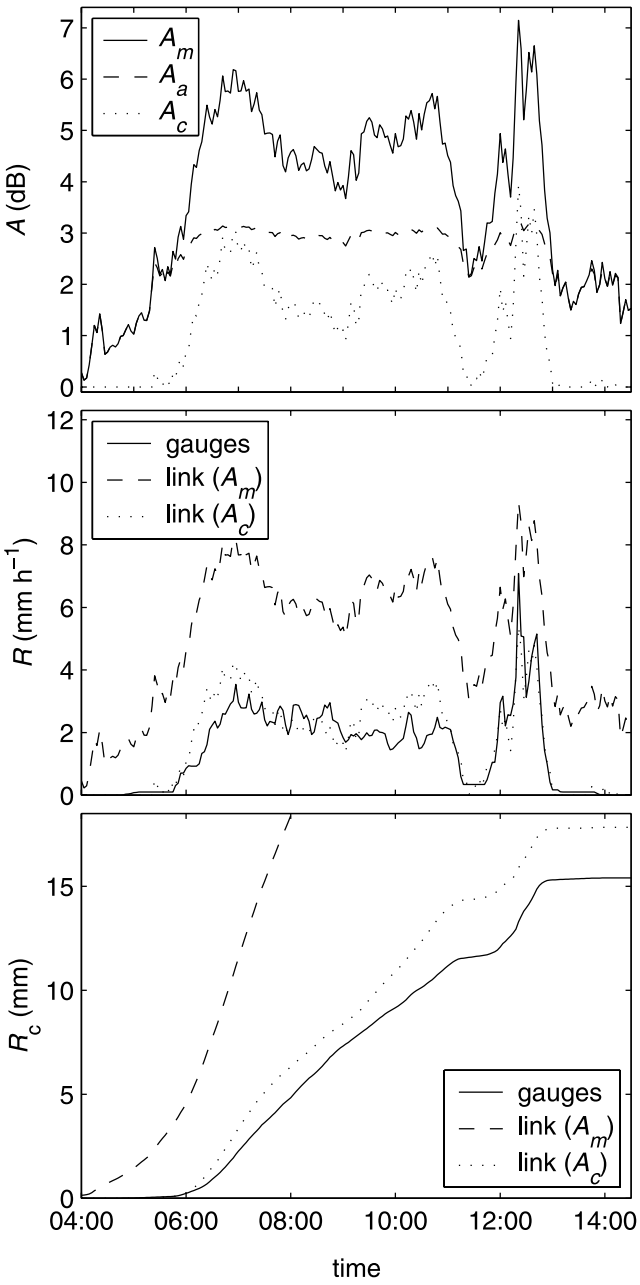

Figure 10. (top) Measured attenuation (A_m), rainfall intensity, and cumulative rainfall measured by the link, (middle and bottom) compared to the rainfall measured by the gauges. Also shown are the wet antenna attenuation (A_a) and its correction (A_c) on 5 June 1999. The cumulative rainfall graph is truncated at 18.5 mm because the value for the uncorrected link rainfall at 1430 is $R_c = 52.8$ mm.

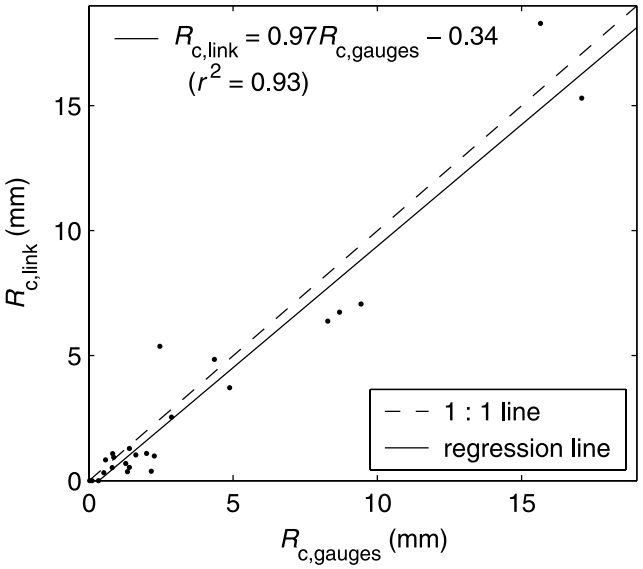

Figure 11. Comparison of the path-averaged cumulative rainfall for all 25 events estimated by the gauges $R_{c,gauges}$ and that estimated using the wet antenna-corrected microwave link signal $R_{c,link}$.

function of the measured attenuation A_m (dB) and time is expressed by *Minda and Nakamura* [2005] as

$$A_a(t) = \max\left\{ \begin{array}{c} \min\left\{ \begin{array}{c} C_1\left(1 - e^{-C_2 A_m(t)}\right) \\ A_m \end{array} \right\} \\ A_a(t_0)e^{-C_3(t-t_0)} \\ 0 \end{array} \right\}, \qquad (13)$$

where t_0 (s) satisfies

$$\min\left\{ \begin{array}{c} C_1\left(1 - e^{-C_2 A_m(t)}\right) \\ A_m \end{array} \right\} < A_a(t_0)e^{-C_3(t-t_0)}.$$

The first (top) part of the wet antenna attenuation function is the attenuation caused by the water films on the antennas during rainfall, and the second part (involving C_3) is that after or in decreasing rain due to the time it takes for the water films to disappear from the antennas. Least squares fitting equation (13) to the residual (k-aR^b)L, where $k \geq 0$, using the data of all the events, leads to such a high value of C_3 that the exponential decay in time does not play a role in practice given the 3-min time step. This means that the wet antenna attenuation is independent of time, so that it can be plotted in Figure 8. The values of the other coefficients are C_1 = 3.32 dB and C_2 = 0.48 dB^{-1}, with a coefficient of determination for the regression of r^2 = 0.65 (values given by *Minda and Nakamura* [2005] are C_1 = 5.0 dB, C_2 = 0.125 dB^{-1} and C_3 = 0.009 s^{-1}; *Kharadly and Ross* [2001] give C_1 = 8.0 dB and C_2 = 0.125 dB^{-1} and state that these values depend on the type of antenna). Hence the maximum wet antenna attenuation is 3.32 dB, which leads to a maximum overestimation of the rainfall intensity of 3.9 mm h^{-1} (occurring at R = 11.6 mm h^{-1}) if no wet antenna correction is applied. The measured attenuation can be corrected for the wet antenna attenuation using

$$A_c = \max\left\{ \begin{array}{c} A_m - A_a \\ 0 \end{array} \right\}, \qquad (14)$$

from which the corrected specific attenuation $k_c = A_c L^{-1}$ can be computed.

[31] Figures 9 and 10 show time series of the attenuation, rainfall intensity and cumulative rainfall R_c(= $\int R\mathrm{d}t$) for two selected events, on 29 May 1999 and on 5 June 1999. The measured attenuation is shown along with the estimated wet antenna attenuation and the corrected attenuation to give an idea of the magnitude of this correction. For the two rainfall variables (Figures 9, middle, 9, bottom, 10, middle, and 10, bottom), the microwave link estimate of the rainfall intensity with and without the wet antenna correction is compared to the gauge-estimated rainfall. It can be seen that the cumulative rainfall estimated by the link without taking into account the wet antenna attenuation is dramatically larger than that estimated by the gauges, especially for an event like that of 5 June 1999, where there is a long period of low-intensity rainfall (and hence a long period where the antennas are wet). Application of the wet antenna correction yields far better results. Because this wet antenna correction depends on the rain gauge measurements, it could be argued that the rainfall intensity estimated using k_c and that estimated from the gauges are not independent. However, considering the fact that the wet antenna correction is based on only two parameters (C_3 does not play a role), fitted for the entire data set, the comparison does provide a good basis on which to test the potential of the instrument to measure precipitation. The dynamics of the rainfall intensity estimated by the gauges and by the link are seen to be very similar for these two events. Hence we can conclude that if the base level of the microwave link signal is known, the microwave link can estimate path-averaged rainfall at a high temporal resolution relatively accurately. As mentioned before, the use of dual-frequency and/or dual-polarization links could significantly reduce the effect of the issue of variable signal base level.

[32] Figure 11 shows the comparison of the total cumulative rainfall for all 25 events measured by the gauges and that estimated from the microwave link, in which the wet antenna attenuation correction was applied. The comparison is seen to be quite good (slope of the linear regression is 0.97, and coefficient of determination r^2 = 0.93), especially for higher accumulations. This again shows that a microwave link is well suited for measuring the path-integrated rainfall, in this case integrated over entire events.

4. Conclusions

[33] The potential for a single-frequency, single-polarization microwave link to measure path-averaged precipitation has been investigated. As shown by other investigators in the past, the relation between the attenuation measured by the microwave link system and the rainfall intensity is seen to be nearly linear and nearly independent of the drop size distribution and the rain temperature at 27 GHz. A power law k-R relation with coefficient a = 0.132 dB km^{-1} (mm h^{-1})$^{-b}$ and exponent b = 1.074 has

been derived from more than a year of measurements of DSDs in the Netherlands, and has been used in this paper.

[34] Results of an experiment carried out in the summer of 1999 in the center of the Netherlands have been used to test whether a microwave link can be used to estimate precipitation. Analyses of data recorded by a microwave link system and a line configuration of seven rain gauges show that it is extremely important to keep the electronics of both the transmitter and the receiver stable, and to either calibrate the antennas for wet antenna attenuation or to avoid wetting of the antennas in the first place, e.g., by using a roof.

[35] We have calibrated the antennas for wet antenna attenuation using a relation from the literature and data recorded by the rain gauges. The path-averaged rainfall intensity estimated using the resulting corrected specific attenuation is shown to represent that estimated by the gauges well, both in magnitude and in dynamics. From these results, we conclude that a microwave link can be used to measure precipitation if it is installed correctly. Combining this with the conclusions from *Leijnse et al.* [2007], we can state that a microwave link has great potential for measuring both evaporation and precipitation.

[36] **Acknowledgments.** The authors would like to thank G. van de Abeele of the Hydrology and Quantitative Water Management Group, Wageningen University, for technical assistance with the microwave instrument, M. H. A. J. Herben and A. C. A. van der Vorst of the Eindhoven University of Technology for their advice regarding the instrument, A. E. Green of the Horticultural Research Institute of New Zealand for lending the instrument, and their colleagues from the Meteorology and Air Quality Group at Wageningen University for providing the temperature and humidity data. H.L. and R.U. are financially supported by the Netherlands Organization for Scientific Research (NWO) through a grant (016.021.003) in the framework of the Innovational Research Incentives Scheme (Vernieuwingsimpuls).

References

Atlas, D., and C. W. Ulbrich (1977), Path- and area-integrated rainfall measurement by microwave attenuation in the 1–3 cm band, *J. Appl. Meteorol.*, *16*, 1322–1331.

Battan, L. J. (1973), *Radar Observation of the Atmosphere*, 324 pp., Univ. of Chicago Press, Chicago, Ill.

Beard, K. V. (1976), Terminal velocity and shape of cloud and precipitation drops aloft, *J. Atmos. Sci.*, *33*, 851–864.

Berne, A., G. Delrieu, J.-D. Creutin, and C. Obled (2004), Temporal and spatial resolution of rainfall measurements required for urban hydrology, *J. Hydrol.*, *299*, 166–179.

Green, A. E., S. R. Green, M. S. Astill, and H. W. Caspari (2000), Estimating latent heat flux from a vineyard using scintillometry, *Terr. Atmos. Oceanic Sci.*, *11*(2), 525–542.

Grum, M., S. Krämer, H.-R. Verworn, and A. Redder (2005), Combined use of point rain gauges, radar, microwave link and level measurements in urban hydrological modelling, *Atmos. Res.*, *77*, 313–321.

Herben, M. H. A. J., (1984), The influence of tropospheric irregularities on the dynamic behaviour of microwave radio systems, Ph.D. thesis, Tech. Hogesch. Eindhoven, Eindhoven, Netherlands.

Holt, A. R., G. G. Kuznetsov, and A. R. Rahimi (2003), Comparison of the use of dual-frequency and single-frequency attenuation for the measurement of rainfall along a microwave link, *IEE Proc. Microwave Antennas Propag.*, *150*(5), 315–320.

Joss, J., J. C. Thams, and A. Waldvogel (1968), The variation of raindrop size distributions at Locarno, paper presented at International Conference on Cloud Physics, Am. Meteorol. Soc., Toronto, Ont., Canada.

Kharadly, M. M. Z., and R. Ross (2001), Effect of wet antenna attenuation on propagation data statistics, *IEEE Trans. Antennas Propag.*, *49*(8), 1183–1191.

Krämer, S., H.-R. Verworn, and A. Redder (2005), Improvement of X-band radar rainfall estimates using a microwave link, *Atmos. Res.*, *77*, 278–299.

Laws, J. O., and D. A. Parsons (1943), The relation of raindrop-size to intensity, *Eos Trans. AGU*, *24*, 452–460.

Leijnse, H., J. A. Smith, and M. L. Baeck (2002), The use of radar rainfall estimates for hydrologic modelling of flood response in urban drainage basins, in *Proceedings of the XIVth International Conference on Computational Methods in Water Resources*, vol. 2, edited by S. M. Hassanizadeh et al., pp. 1371–1378, Elsevier, New York.

Leijnse, H., R. Uijlenhoet, and J. N. M. Stricker (2007), Hydrometeorological application of a microwave link: 1. Evaporation, *Water Resour. Res.*, *43*, W04416, doi:10.1029/2006WR004988.

Marshall, J. S., and W. M. Palmer (1948), The distribution of raindrops with size, *J. Meteorol.*, *5*, 165–166.

Minda, H., and K. Nakamura (2005), High temporal resolution path-average raingauge with 50-GHz band microwave, *J. Atmos. Oceanic Technol.*, *22*, 165–179.

Mishchenko, M. I., and L. D. Travis (1994), T-matrix computations of light scattering by large spheroidal particles, *Opt. Commun.*, *109*, 16–21.

Olsen, R. L., D. V. Rogers, and D. B. Hodge (1978), The aR^b relation in the calculation of rain attenuation, *IEEE Trans. Antennas Propag.*, *26*(2), 318–329.

Pruppacher, H. R., and J. D. Klett (1997), *Microphysics of Clouds and Precipitation*, 2nd ed., Springer, New York.

Rahimi, A. R., A. R. Holt, G. J. G. Upton, and R. J. Cummings (2003), The use of dual-frequency microwave links for measuring path-averaged rainfall, *J. Geophys. Res.*, *108*(D15), 4467, doi:10.1029/2002JD003202.

Rahimi, A. R., G. J. G. Upton, and A. R. Holt (2004), Dual-frequency links—A complement to gauges and radar for the measurement of rain, *J. Hydrol.*, *288*, 3–12.

Rincon, R. F., and R. H. Lang (2002), Microwave link dual-wavelength measurements of path-average attenuation for the estimation of drop size distributions and rainfall, *IEEE Trans. Geosci. Remote Sens.*, *40*(4), 760–770.

Ruf, C. S., K. Aydin, S. Mathur, and J. P. Bobak (1996), 35-GHz dual-polarization propagation link for rain-rate estimation, *J. Atmos. Oceanic Technol.*, *13*, 419–425.

Smith, J. A., and W. F. Krajewski (1993), A modeling study of rainfall rate–reflectivity relationships, *Water Resour. Res.*, *29*(8), 2505–2514.

Smith, J. A., M. L. Baeck, J. E. Morrison, P. Sturdevant-Rees, D. F. Turner-Gillespie, and P. D. Bates (2002), The regional hydrology of extreme floods in an urbanizing drainage basin, *J. Hydrometeorol.*, *3*(3), 267–282.

Ulaby, F. T., R. K. Moore, and A. K. Fung (1981), *Microwave Remote Sensing: Active and Passive*, vol. I, *Microwave Remote Sensing Fundamentals and Radiometry*, Addison-Wesley.

Upton, G. J. G., A. R. Holt, R. J. Cummings, A. R. Rahimi, and J. W. F. Goddard (2005), Microwave links: The future for urban rainfall measurement?, *Atmos. Res.*, *77*, 300–312.

van de Hulst, H. C. (1957), *Light Scattering by Small Particles*, 470 pp., John Wiley, Hoboken, N. J.

Wessels, H. R. A. (1972), Measurements of raindrops in De Bilt (in Dutch), *Tech. Rep. 72-06*, R. Neth. Meteorol. Inst., De Bilt.

H. Leijnse, J. N. M. Stricker, and R. Uijlenhoet, Hydrology and Quantitative Water Management, Wageningen University, Droevendaalsesteeg 4, 6708 PB Wageningen, Netherlands. (hidde.leijnse@wur.nl)